APPLICATION OF A NUMERICAL MODEL TO LAKE VÄNERN

by T J Simons, L Funkquist and J Svensson

SMHI Rapporter

HYDROLOGI OCH OCEANOGRAFI

Nr RHO 9 (1977)

SVERIGES METEOROLOGISKA OCH HYDROLOGISKA INSTITUT

APPLICATION OF A NUMERICAL MODEL TO LAKE VÄNERN

by T J Simons, L Funkquist and J Svensson

SMHI Rapporter

HYDROLOGI OCH OCEANOGRAFI

Nr RHO 9 (1977)

TILLÄMPNING AV EN NUMERISK MODELL PÅ VÄNERN

SVERIGES METEOROLOGISKA OCH HYDROLOGISKA INSTITUT

Norrköping 1977

ABSTRACT

Current, temperature and water-level measurements in Lake Vänern from two episodes in 1971, representing a stratified resp an unstratified situation, have been used for the verification of a multi-layer hydrodynamic model. Concentrating on wind-driven lake circulation it is shown that, aside from the currents along the western shore of the eastern basin, the correspondence between model results and observations is satisfactory. The computed currents could therefore be used for studies on the transport and dilution of waste-water in the lake. It is also concluded that neither a variation of model parameters nor an increased vertical or horizontal resolution will make the model reproduce the strong and mainly south-going current along the western shore of the eastern half of the lake.

SAMMANFATTNING

Verifiering av en flerlagers hydrodynamisk modell tillämpad på Vänern har utförts med hjälp av ström-, temperatur- och vattenståndsvärden från två perioder 1971 (representerande skiktade resp oskiktade förhållanden). De beräknade strömmarna visas stämma väl överens med observerade data och bör därför kunna utgöra ett bra underlag vid studier av transportvägar och utspädningsgrad för olika typer av utsläpp. De relativt starka strömmarna i västra delen av Värmlandssjön har inte kunnat beskrivas i modellen trots försök med flera kombinationer av modellens parametervärden och ökad horisontell och vertikal upplösning.

CONTENTS

FIGURES

FIGURER

1. INTRODUCTION

Lake Vänern, the largest lake in Sweden, with a volume of 150 km^3, has received increasing attention as a fresh water reservoir, recreation area and fishing-ground as well as a waste-water recipient and navigable passage. It is polluted in the north by the pulp mill industry and in the south by small rivers from the densely populated farming district. The yearly amount of fresh water supplied is about 17 km^3 of which 5.2 km^3 is discharged from the nonpolluted Klarälven in the northeastern part of Lake Vänern.

The lake is divided into two basins which are connected by a shallow sound. The maximum depth is about 100 m and situated in the eastern basin. The western basin has a depth of about 70 m.

The inflow of wastes is mainly into the northeastern part of the lake. This has created a significant difference in water quality between the two basins. Until the beginning of the 1960's, the effluents were becoming increasingly polluted but later because of the closing of factories and cleaner industrial processes this trend was stopped and pollution has been decreasing ever since.

The water quality which earlier was rather bad has since 1970 steadily grown better.

An intense research program was started by SMHI in 1971 to study the circulation and temperature structure of the lake. Extensive field measurements were carried out and model studies of the lake were undertaken.

The computed pictures of the lake's circulation under different weather conditions can after verification form a base for studies of the transport and dilution of waste water from sources ashore.

Financial support for the project came from Swedish Environment Protection Board and from SMHI.

2. MEASUREMENT PROGRAM AND DATA ANALYSIS

The measurements during spring 1971 were the beginning of an extensive mapping of the dynamics and the variations of physical and chemical parameters in Lake Vänern. In the following the measurements of interest for verification of the numerical model will be briefly summarized.

Automatic Aanderaa current meters were placed at 7 stations (for location see Fig 1). The reliability of the current meters and their vertical positions are shown in Fig 2. Temperature was recorded at 11 levels at 6 stations with thermistor chains also manufactured by Aanderaa. Timesteps of 10 and 20 minutes were used for current resp temperature recordings. At the strait joining the two parts of the lake some additional measurements of the same kind were made during two periods of 14 days, partly coinciding with the first verification period.

Water level was continually recorded at 3 permanent stations P4, P7 and P9, whose location is shown in Fig 1. During the verification periods 6 additional gauges were working at stations P1, P2, P3, P5, P6 and P8.

Comparison between model results and field records is based on currents, temperatures and water levels for two selected episodes, each lasting 10 days. Records from the 1971 measurement program were extracted to correspond to the two episodes when the model was run. These data sets then were analysed in the same way as the model output.

Magnitude and direction of the current were recorded every 10th minute and the values closest to the exact hour were used for time series of hourly values. After smoothing with a low-pass filter, only waves with periods longer than 14-18 hours remained in the series. As the intertial waves at the latitude of Lake Vänern have a period of about 14 hours, the filtered series represent the large-scale changes of the lake circulation. As the aim of this study is to get a knowledge of the net transport rather than a full description of the small-scale behaviour of the current, it is natural to concentrate on time and space scales corresponding to meteorological changes like passing fronts. The inertial waves will however be discussed in the last chapter.

The currents from the different layers of the model were compared to current meter data from 7, 15, 25 and 40 m. No interpolation was made to get recorded values to correspond to the layer division of the model.

Temperature records were analysed in analogy with the current meter data. Recorded temperatures served as a basis for partly defining the initial state of the lake when the model runs started. As the layer division of the model is relatively coarse there was no reason to try a detailed description of the thermocline behaviour. Nor has the horizontal variation of temperature been included in the initial state of the model.

Observations of surface pressure and windstress are taken every third hour at a few stations around Lake Vänern. Alone they are insufficient to give a good picture of the windfield over the lake. Therefore routine analyses of 3-hourly synoptic weather maps were further analysed to show the windfield. In this manner winds for five fictitious stations, each representing a specified area of the lake surface, were obtained. Quadratic interpolation in time then produced the half-hourly values used as continous input to the model.

Objective methods are insufficient and hardly suited for the present kind of model verification. Instead a subjective way of studying time series from field measurements and corresponding gridvalues from the model is used. In verifying the currents the time series are of two kinds: one with vector plots and the other with plots of both magnitude and direction. Instantaneous pictures of the modeled circulation of the whole lake are also of interest. The pictures still contain near-inertial waves and the represented currents in the surface layer are strongly dependent on water depths. But in this way the reaction of the lake to different wind situations and bottom topography effects can be partly studied. The recorded currents are also plotted on these charts. They are not to be used either for verification nor corrections to the modeled circulation. Possible phase-differences in short-periodic waves in both kind of data may be sufficient to create large deviations in both magnitude and direction.

3. NUMERICAL MODEL

The mathematical model extends the framework of the familiar storm surge model to include a description of the three-dimensional current and temperature distributions in the lake. The model employs the hydrodynamical-numerical methods developed in the context of numerical weather forecasting and subsequently applied to oceanographic problems (see e.g., Bryan, 1969). The governing equations are the principle of mass conservation, the equations of motion, and the thermodynamic energy equation. A number of approximations are introduced in this basic set of physical relationships. It is assumed that vertical accelerations can be neglected and that the flow is quasi-hydrostatic. Density variations are ignored except where they influence buoyancy so that the water is effectively imcompressible. Effects of motions smaller than the numerical grid scale are incorporated in the form of mixing coefficients. These mixing processes are simulated in analogy to the gradient diffusion concept such that turbulent friction and heat diffusion are parameterized by eddy viscosities and diffusivities. Using these approximations, the equations of motion, the first law of thermodynamics, and the mass continuity condition can, respectively, be written as follows

$$\frac{\partial u}{\partial t} + \nabla . (\underset{\sim}{v} u - A_H \nabla u) + \frac{\partial}{\partial z} (wu - A_V \frac{\partial u}{\partial z}) = fv - \frac{\partial}{\partial x} (P + Q) \qquad (1)$$

$$\frac{\partial v}{\partial t} + \nabla . (\underset{\sim}{v} u - A_H \nabla v) + \frac{\partial}{\partial z} (wv - A_V \frac{\partial v}{\partial z}) = -fu - \frac{\partial}{\partial y} (P + Q) \qquad (2)$$

$$\frac{\partial T}{\partial t} + \nabla . (\underset{\sim}{v} T - K_H \nabla T) + \frac{\partial}{\partial z} (wT - K_V \frac{\partial T}{\partial z}) = 0 \qquad (3)$$

$$\frac{\partial w}{\partial z} = - \frac{\partial u}{\partial x} - \frac{\partial v}{\partial y} \qquad (4)$$

where t is time, x and y are the horizontal coordinates, z is the vertical coordinate measured upward, ∇ is the horizontal gradient operator, u, v, w are the velocity components along the three coordinates, $\underset{\sim}{v}$ is the horizontal velocity vector, and T is temperature. A_H and A_V represent the horizontal and vertical eddy viscosities, K_H and K_V are the corresponding heat diffusivities, f denotes the Coriolis parameter, and P and Q represent barotropic and baroclinic pressure components defined below

$$P = g\zeta + P_s/\rho_o \quad Q = g \cdot \int_z^{\zeta} \frac{\Delta\rho}{\rho_o} dz \qquad (5)$$

where ζ denotes the free surface elevation, g is the earth's gravitational acceleration, P_s is the atmospheric pressure at the air-sea interface, ρ_o is the mean water density, and $\Delta\rho$ is the density anomaly. For fresh water the latter can be related to temperature by the simple quadratic expression

$$\frac{\Delta\rho}{\rho_o} = -6.8\ 10^{-6} (T - 4^o)^2 \qquad (6)$$

where T is given in degrees centigrade (see, e.g., Simons, 1973).

The continuity equation (4) serves to compute the vertical velocity from the horizontal flow divergence, by recourse to the lower boundary condition that the flow normal to the bottom must vanish. Vertical integration of the same equation results in the conventional prediction equation for the free surface elevation, which determines the barotropic pressure function (5). If the short-term variations associated with free surface oscillations are not considered of interest, the latter equation can be used to define a streamfunction for the vertically-integrated flow, which can be predicted from the vorticity equation for this flow. In the present model, the free surface prediction is included for comparison with water level observations.

Boundary conditions for fluxes of momentum and heat normal to the free surface and the bottom are

$$\rho A_V \frac{\partial u}{\partial z}\Big|_s = \tau_{sx} \qquad \rho A_V \frac{\partial v}{\partial z}\Big|_s = \tau_{sy} \qquad \rho K_V \frac{\partial T}{\partial z}\Big|_s = q_s$$

$$\rho A_V \frac{\partial u}{\partial z}\Big|_b = \tau_{bx} \qquad \rho A_V \frac{\partial v}{\partial z}\Big|_b = \tau_{by} \qquad \rho K_V \frac{\partial T}{\partial z}\Big|_b = 0$$

where τ_s and τ_b are the surface windstress and the bottom drag, respectively, and q_s is the downward surface flux of heat. The windstress and bottom drag are related to surface winds and bottom currents by the conventional quadratic stress laws, while the heat flux is specified in terms of external parameters. Finally, at the lateral boundaries the normal components of temperature fluxes and current must vanish, while the tangential velocity component will be subjected to free-slip or no-slip conditions depending on the type of model.

Numerical solutions of the above equations are obtained by finite-difference methods, with the variables being distributed on a staggered grid. In a horizontal plane, the free surface, the vertical velocity and the temperature are located at the center of gridsquares, whereas horizontal currents are defined at the boundaries of these squares. Two types of models are utilized. In the first case, normal velocity components are specified at the sides of a grid square and hence the two horizontal velocity components are not available at the same points. This is the single lattice model which has been found very useful for storm surge forecasting, although it has the disadvantage that the Coriolis terms must be averaged over four points and thus allows for spurious inertial frequencies. In this model the tangential velocity components never coincide with the shores and it is most convenient to impose free-slip lateral boundary conditions. The second type of model has a double-lattice structure with both velocity components defined at the corners of the grid squares. In this case the tangential velocity along the shores is set equal to zero together with the normal velocity. This type of model requires some form of lateral smoothing to prevent lattice dispersion problems (see, e.g., Platzman, 1963).

The vertical structure of the multi-layered model consists of a system of fixed horizontal levels where the vertical movement of the water is calculated. This procedure appears more convenient than moving material interfaces when dealing with high vertical

resolution and irregular bottom topography. The levels are spaced apart by arbitrary intervals along the vertical. Vertical velocities, stresses and vertical fluxes are computed for each level, whereas temperature and current are defined as averages for the intermediate layers. The layered system of equations is transformed into an equivalent system consisting of one equation for the vertically-integrated flow and a set of equations for the shearing flow between adjacent model layers. This procedure effectively eliminates the effects of the free surface oscillations on the internal flow computations and therefore the latter are not subjected to the stability condition associated with time extrapolation of the former. All time extrapolations are carried out by explicit methods except for the Coriolis term which is treated by an implicit scheme. Central time differences are employed for pressure-divergence terms and forward differences for friction-diffusion terms. Nonlinear terms are treated by a two-step method similar to the Lax-Wendroff scheme. A more detailed discussion of the physical and numerical approximations employed in the model, has been presented by Simons (1973).

4. MODEL VERIFICATION

Two episodes during the 1971 field measurement program were selected to test the model. During the first period, Aug 26 - Sept 4, the lake was stratified with a well-defined thermocline. During the second episode, Oct 31 - Nov 9, the lake was homogeneous and well-mixed in the vertical. The episodes will be referred to as "stratified" and "homogeneous", respectively. Since the homogeneous lake is presumably easier to model than a stratified situation, the second episode was actually studied first and it seems logical to discuss the results in the same order.

Initially, a four- layer model was selected with a horizontal resolution of 5 km. The timestep for the free-surface prediction was 3 min and the timestep for the internal flow prediction was taken to be 15 min. The windstress coefficient was set at $2.5 * 10^{-3}$ and a similar value was adopted for the bottom drag coefficient. The homogeneous computations were carried out on a double lattice grid with a horizontal eddy viscosity of 10^6 cm^2/s, while the vertical eddy viscosity varied between 50 and 250 cm^2/s. The nonlinear inertial terms were neglected. Initial simulations for the stratified episode were carried out with the same model but including temperature predictions with eddy diffusivities of 10^5 cm^2/s in the horizontal and 1 cm^2/s in the vertical. Subsequently, a variety of model configurations and parameters were applied to the stratified lake to investigate if any of the shortcomings of the initial simulations could be remidied. A detailed comparison of these results will be presented in the next section. The present discussion is devoted to a general verification of the initial model results.

The two verification episodes were naturally selected for their interesting meteorological conditions, so that it would be easier to study the response of the lake to windforcing. Considering first the homogeneous period (31.10 - 9.11), the weather was initially dominated by a cold front passing eastwards over northern Europe after a prolonged period of high pressure. After the first few days, weakly developed ridges interrupted the effects of passing fronts. A deep low whose center passed almost over the lake, caused considerable changes in winds on Nov 6. Winds for this episode are shown at the centre of Fig 3 at interval of 3 hours.

The model verification for the homogeneous period is concerned with water levels and currents. The primary purpose of the water level comparison is to verify that the wind stress coefficient is properly estimated. There are nine water level stations situated around Lake Vänern as shown in Fig 1. For comparison with the model results, Fig 3 shows observed and computed water levels for two stations along the NE shore and two stations along the SW shore. The agreement between model results and observations is good except for Nov 6. Since the observed setup at this time is much larger than computed, one would conclude that the wind was probably more from the NE instead of the SE as shown in the figure. Since the amplitudes of the surface variations are otherwise of the right magnitude, it is assumed that the stress coefficient is acceptable.

The current verification is based on the observations listed in Fig 2. In the first experiment the model layers were separated at levels of 10, 25 and 50 m below the surface and the vertical eddy viscosity was 50 cm^2/s. It was quite apparent that the model produced much larger near-inertial oscillations in the currents than the observations showed. The vertical eddy viscosity was therefore increased to 250 cm^2/s in the next experiment. As will be seen in the next section, this tends to reduce short-term current oscillations without causing essential changes in the long-term solutions. Now the current speeds are reasonably well simulated but the directions are sometimes in error by up to 90 degrees. Examples are shown in Fig 4.

The computations were repeated with different positions of the model layers, but the effects of this change were minor. It was decided to concentrate on the more interesting stratified period for a complete series of modeling experiments.

An interesting weather situation during 26.8 - 4.9 was the reason for choosing this period to represent a stratified situation. Both days of weak winds, when the lake could adapt itself to a rather unaffected situations, and days with increasing winds were found during this period.

A study of weather-bulletins shows the importance of an extensive high for the large-scale atmospheric circulation up to 27.8. (A description of the wind for the centre of Lake Vänern is shown in Fig 5). The lows passed north of Scandinavia and winds over the lake were changing and seldom reached 8 m/s. The high was gradually weakening and the rest of the period was characterized by a series of passing-lows. The wind was mainly from south or west and only 30.8 colder air from the north was advected behind a front.

The stratified model has initially four layers separated at 10, 20 and 35 m below the surface. The initial temperature was uniform in the horizontal and varied from 17 °C in the upper layer to 7 °C in the lower layer. A typical vertical temperature distribution for the stratified period is shown at the bottom of Fig 5. On the basis of the extensive series of experiments discussed in the following section, it appeared that four layers would be sufficient to produce an acceptable simulation. Thus the present discussion of model verification is based on a four-layer model with a vertical eddy viscosity of 100 cm^2/s. It will be shown later which effects result from different coefficients.

In Fig 6a, b and c time series of current vectors from three stations near the coast in the eastern basin are plotted. Locations of the three stations are shown in Fig 1. Station D shows that the model is quite capable of describing the southern part of the general cyclonic circulation of the lake. In the first days with weak winds the measured data show a circulation that is clearly the result of previous disturbances. As the model starts from rest it needs a certain time with a marked windstress to compute a circulation pattern that corresponds to the real one. From the vector plots it seems that a good agreement is reached already on the third day, though the first two days were very calm. During

the rest of the period there is good agreement in both magnitude and direction. The weakening currents on 30.8 must be related to the only occasion with northern winds and probably the short-term wind from the north didn't influence the current at 7 m depth to the same extent as they affected the upper layer of the model, which represents the integrated current from the surface down to 10 m.

At the strait that divides the lake into two parts the circulation is rather complicated. The current at station F and G often runs in different direction i e NE or SW currents at F are mostly related to NW resp SE currents at G. Here only results from station G will be shown. The agreement again is very good and the prevailing westgoing current, almost against the wind, only changes during 30.8. Then the aforementioned wind causes small turning and decrease in magnitude of the currents which appears a little earlier in the measurements than in the model results. It is probably not due to a timelag in the windstress but the relatively strong current before the decrease in magnitude points to an overestimate of the circulation in the surrounding area.

Looking at station C it is difficult to find any resemblance between model and data. The measured and empirically known strong southgoing current is closely related to the upwelling along the coast which is also confirmed by more detailed measurements in 1972. To explain the model results one could argue that although the current is increasing during storms, it never tends to zero thus indicating that the current has a relatively long history. A simulation of ten days, starting form rest therefore does not seem to be adequate to produce this part of the lake circulation. It is likely that a proper simulation of currents along the western shore is only possible if the initial circulation and horizontal density structure are included in such short-term modeling experiments. At any rate, it will be shown later that different model resolutions and parameters do not lead to essential improvement of these results.

The character of the comparisons between model results and observations at the remaining stations A, B, F and H and the lower layers at station D is not significantly different from what is shown in Fig 6a and b. Therefore the conclusion of the current verification for the stratified period is that the model simulation of the long-term pattern of the lake circulation is in good agreement with observations with the exception of the strong currents along the western coast of the eastern basin.

Synoptic pictures of currents from each layer were plotted along with the recorded values (Fig 7a and b). As mentioned before attention should be paid to the momentary character of the plotted circulation. Here only current maps from one instant, 1.9.1971 at time 00.00, will be discussed. Under the influence of the mostly S to SW winds from the previous two days a general cyclonic circulation had developed in the eastern basin. The same pattern is computed for the other layers. As an example the result from the third layer is shown. In the upper layer of the western basin there is a mean current to the north, rather weak in the middle but stronger along the shore. The water is returning in the third

layer thus giving different types of circulation in the two parts of the lake. The model also tells that there is a great exchange of water between the two parts with a mixing of the upwelling water from an underwater canyon east of the strait. The far too weak currents in isolated gridareas like the NW part of the lake and the long and shallow bays are effects of the course resolution of bottom topography and shorelines in the model.

To illustrate the quality of temperature predictions, Fig 8 shows observed temperatures at a depth of 25 m for the stations in the eastern half of the lake, together with model results. In this case, an 8-layer model was used with a vertical eddy viscosity of 50 cm^2/s for all stations, except station C, for which a lower eddy viscosity gives better agreement with observations. This will be discussed in more detail in the next section. The figure illustrates that the time variations of temperature show the same character in the model and in the real lake. Thus stations A and B indicate downwelling, station C shows pronounced short-term oscillations, and station D displays waves of longer periods. At the same time it is clear that a detailed comparison shows considerably differences between model results and observations.

5. VARIATION OF MODEL STRUCTURE

The stratified episode, Aug 26 - Sept 4, has been simulated by a variety of model structures, resolutions, and parameters, in order to investigate which type of model would best simulate the observed phenomena in Lake Vänern. This series of experiments is summarized in Table 1. With regard to model structure, two types of grids were used, namely, a single lattice (SL) and a double lattice (DL), as discussed in section 3. Some computations on the double lattice grid included the nonlinear (NL) advection terms in the equations of motion. The experiments indicated by an asterisk were carried out with a homogeneous model as well as with the stratified model. With regard to resolution, the horisontal grid mesh varied from 2.5 to 5 km and the number of layers varied from 4 to 8. In the 4-layer models, the layers were separated by horizontal levels at 10, 20, and 35 m below the surface. In the 6-layer version the levels were at 10, 17, 20, 23, and 35 m, thus allowing for a better representation of the thermocline. In the 8-layer model the levels were 10, 17, 22, 27, 33, 40, and 50 m. With regard to model parameters, different values were considered for horizontal and vertical eddy viscosities (A_H, A_V) and the corresponding eddy diffusivities of heat (K_H, K_V). The vertical eddy viscosity was taken to decrease from a maximum at the surface, presented in the Table, to half that value at the thermocline and below.

A discussion of current simulations must differentiate between different frequencies, in particular, between near-inertial oscillations and long-term variations. The inertial period for lake Vänern is approximately 14 hrs and thus a digital filter with a cut-off at 15 hrs was used to separate all observed and computed currents into a low-pass and a high-pass series. If this is done, it becomes clear that the most pronounced results of model variations are the effects of vertical eddy viscosity on the near-inertial oscillations. This is illustrated in Fig 9 which presents observed high-pass current for station B together with model results for vertical eddy viscosities of 50 and 10 cm^2/s, respectively. All stations, except station C, show the same behaviour as station B, thus indicating that the higher eddy viscosity is to be preferred. On the other hand, station C shows consistently higher amplitudes in the near-inertial range, which are best simulated by the lower eddy viscosity. This is illustrated in Fig 10. Although the vertical structure of the short-term fluctuations may be altered by a different model configuration or resolution, none of these effects are comparable to the above.

The primary purpose of the present modeling project is to simulate water movements on a longer time scale and hence our discussion will concentrate on that. At the outset it should be noted that the low-pass currents show no dramatic variations as a function of either model structure or model parameters. However, some systematic differences become apparent and, rather than reviewing the whole series of experiments, a few examples will be taken to illustrate these changes. Since station C showed the least agreement between model results and observation, it appears of particular interest to concentrate on this station.

Considering first the change from a double-lattice to a single-lattice model, it is generally found that the nearshore currents become larger in the second model. This was to be expected because the tangential velocity is forced to go the zero at the lateral walls of the double-lattice model, whereas the single-lattice model imposes such a condition only on the normal component. Since the majority of the present stations are located close to the shores of the lake, the low-pass currents tend to be larger in the single-lattice models. The directions, however, remain generally the same. To illustrate this effect, Fig 11 shows filtered currents for station C as obtained from a single and a double lattice model, respectively, for the same resolution and parameters. The southerly flow is somewhat increased in the single lattice model but still much smaller than observed.

Effects of increased resolution are considerably less than proportional to the increase in computing effort, at least in regard to current simulations. In effect, the additional information resulting from a smaller grid or a larger number of layers is in general not different from that which would be obtained by interpolation results from a coarser grid. There is no doubt that high resolution is required to simulate near-shore processes in a stratified lake, in view of the small radius of deformation of the thermocline. However, for the present observation stations, no improvement in model performance could be detected after the resolution was increased. The same conclusions also apply to the nonlinear inertial terms in the equations of motion. Again the computational effort is greatly increased without a corresponding improvement in model verification.

The present series of experiments again appear to confirm the conclusion that mixing parameters are the primary means to affect model solutions. Among these, the vertical eddy viscosity is the most important one since it effectively determines the vertical current profile. Comparison of simulations with and without heat diffusion in the horizontal or vertical failed to show any effects for the time scales considered here. Horizontal eddy viscosities of the order of magnitude included here, lead to minor changes in the open lake but can result in reduced current speeds in the nearshore zones. However, the effect is closely linked to the type of lateral boundary condition and the lattice structure of the grid, which determines where the velocity points are defined in relation to the shore. Again taking station C as an example, Fig 12 a shows results from a single lattice 4-layer model with and without horizontal eddy viscosity. Finally Fig 12 b illustrates effects of vertical eddy viscosity on low-pass currents. The differences are not comparable to those for the high-pass currents shown in Fig 10, but they are not negligible. Again, this effect cannot be separated completely from model configuration and other parameters. For instance, variations of vertical eddy viscosity appear to lead to more pronounced changes of computed currents in single lattice models without horizontal viscosity than in double lattice models with horizontal smoothing.

Considering next the temperature predictions, it is clear that they are influenced by the quality of the current simulations as well as by the vertical resolution by which the thermocline is represented. To illustrate the latter, Fig 13 presents temperature predictions for station C as obtained from the 4-layer model and the 8-layer model, respectively. The coefficients are the same in both cases, namely, A_V = 10 cm^2/s and $A_H = K_H = K_V = 0$. The solutions from both models show the same tendency for the layer temperatures to converge, which means that the thickness of the thermocline layer tends to increase. However, the short-term variations are much larger for the high-resolution model because the vertical temperature gradients are better represented. Thus the same vertical motion results in larger temperature changes in the 8-layer model than in the 4-layer model. These temperature waves are connected with the near-intertial current oscillations and hence the amplitudes depend on the vertical eddy viscosity. Thus, temperature predictions from the same type of model by a vertical eddy viscosity of 50 cm^2/s, show a simular variation over a 10-day period but they display essentially no short-term oscillations.

The conclusion of this series of experiments with varying model configurations and parameters is that the basic character of the model results does not change, in particular when dealing with slowly varying currents. In fact, the changes of results between different experiments are mostly predictable and relatively small. Thus the results of this experiment do not seem to indicate a need for very expensive, nonlinear, high resolution models, when dealing with lake-wide circulations. The more economical model discussed in the previous section appears to produce a quite comparable verification.

TABLE 1. Summary of model experiments for stratified episode, Aug 26 - Sept 4. DL = double-lattice grid; SL = single-lattice; NL = nonlinear inertial accelerations; asterisk indicates barotropic plus barocline simulation. Grid spacing given in km and levels of 4-layer model located at depths of 10, 20, 35 m, for 6-layer model at 10, 17, 20, 23, 35 m and for 8-layer model at 10, 17, 22, 27, 33, 40, 50 m.

A_H and A_V are horizontal and vertical eddy viscosities in cm^2/s, K_H and K_V are corresponding heat diffusivities. A_V varies from maximum at the surface, given in the Table, to half that value at the thermocline level.

Run	Model	Grid	Layers	A_V	A_H	K_V	K_H
1	DL	5.0	4	100	10^6	0.1	10^5
2	DL	5.0	4	50	10^6	0.1	10^5
3	DL*	5.0	4	10	10^6	0.1	10^5
4	DL	5.0	4	10	10^5	0.1	10^4
5	DL	2.5	6	100	10^6	0.1	10^5
6	NL*	5.0	4	50	$5 \cdot 10^6$	0.1	10^5
7	NL*	5.0	4	10	10^6	0.1	10^5
8	SL	5.0	4	50	10^6	0.1	10^5
9	SL	5.0	4	50	10^6	0.0	0
10	SL	5.0	4	50	0	0.0	0
11	SL	5.0	4	10	0	0.0	0
12	SL*	5.0	8	50	0	0.0	0
13	SL	5.0	8	10	0	0.0	0
14	SL*	2.5	8	50	10^6	0.0	0
15	SL*	2.5	8	10	0	0.0	0

REFERENCES

Bryan, K, 1969: A numerical method for the study of ocean cirkulation. J Computat. Phys., 4, 347-376

Platzman, G W, 1963: The dynamical prediction of wind tides on Lake Erie. Meteor. Monogr., 4, No 26, 44 pp

Simons, T-J, 1973: Development of three-dimensional numerical models of the Great Lakes. Environment Canada, Ottawa, I.W.D. Scientific Series No 12, 26 pp

DEPTH CONTOURS OF LAKE VÄNERN AND POSITIONS OF MEASUREMENT STATIONS

FIGURE 1

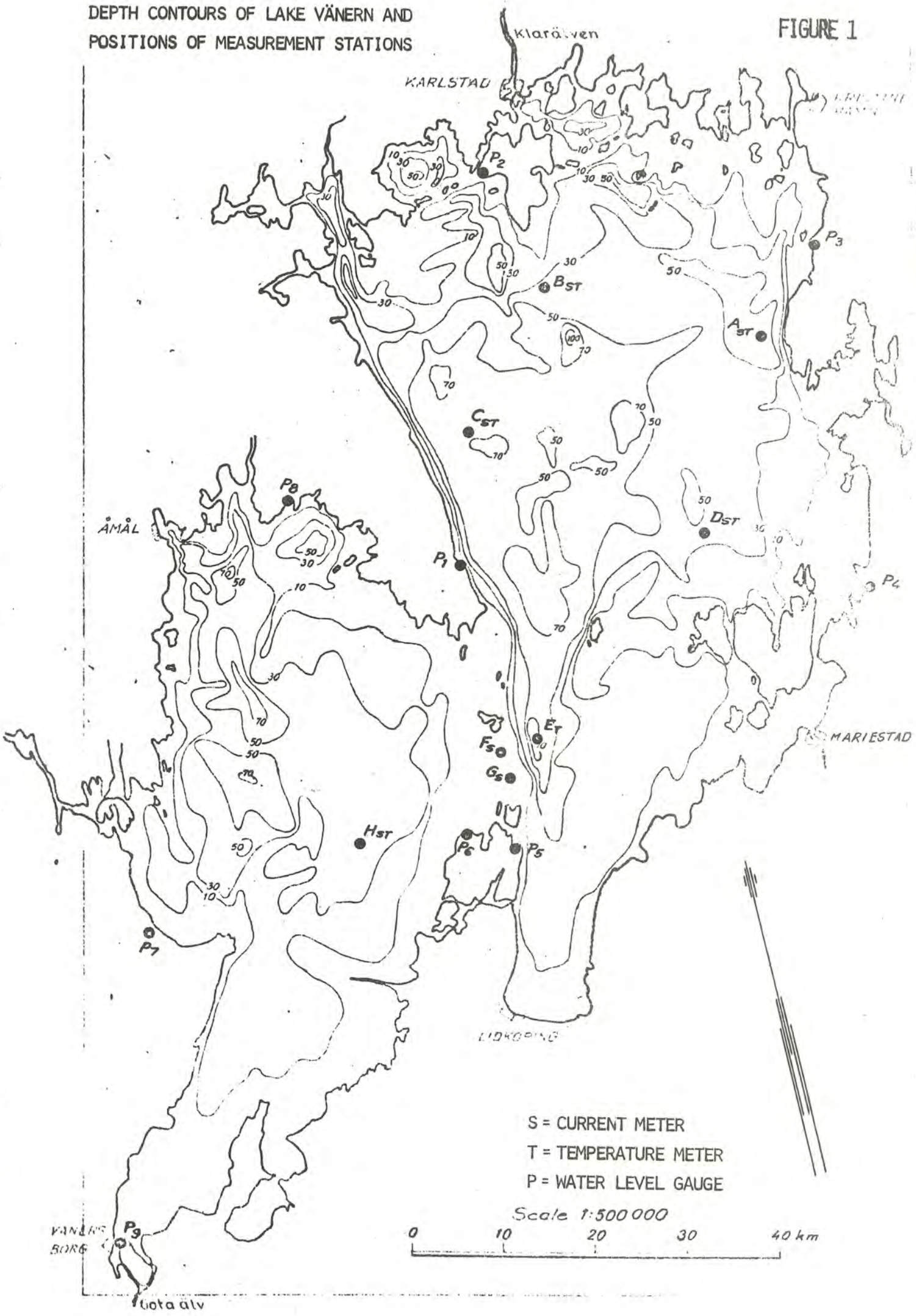

SATISFACTORY RECORD

NOT SATISFACTORY RECORD

Station

A current 7m
25m
temperature

B current 7m
25m
temperature

C current 7m
15m
25m
40m
temperature

D current 7m
25m
temperature

E temperature

F current 7m

G current 10m

H current 7m
25m
temperature

stratified modelling episode

homogeneous modelling episode

MAY | JUN | JUL | AUG | SEP | OCT | NOV | DEC

CURRENT AND TEMPERATURE RECORDS AVAILABLE FROM MEASUREMENT PROGRAM. SELECTED VERIFICATION EPISODES INDICATED BY SHADED AREAS

SMHI HBO

FIGURE 2

S M H I H B O	OBSERVED (SOLID LINES) AND COMPUTED (DASHED) WATER LEVELS FOR SELECTED STATIONS DURING HOMOGENEOUS VERIFICATION EPISODE, TOGETHER WITH WINDS AT INTERVALS OF 3 HOURS	FIGURE 3 1971-11-01--08

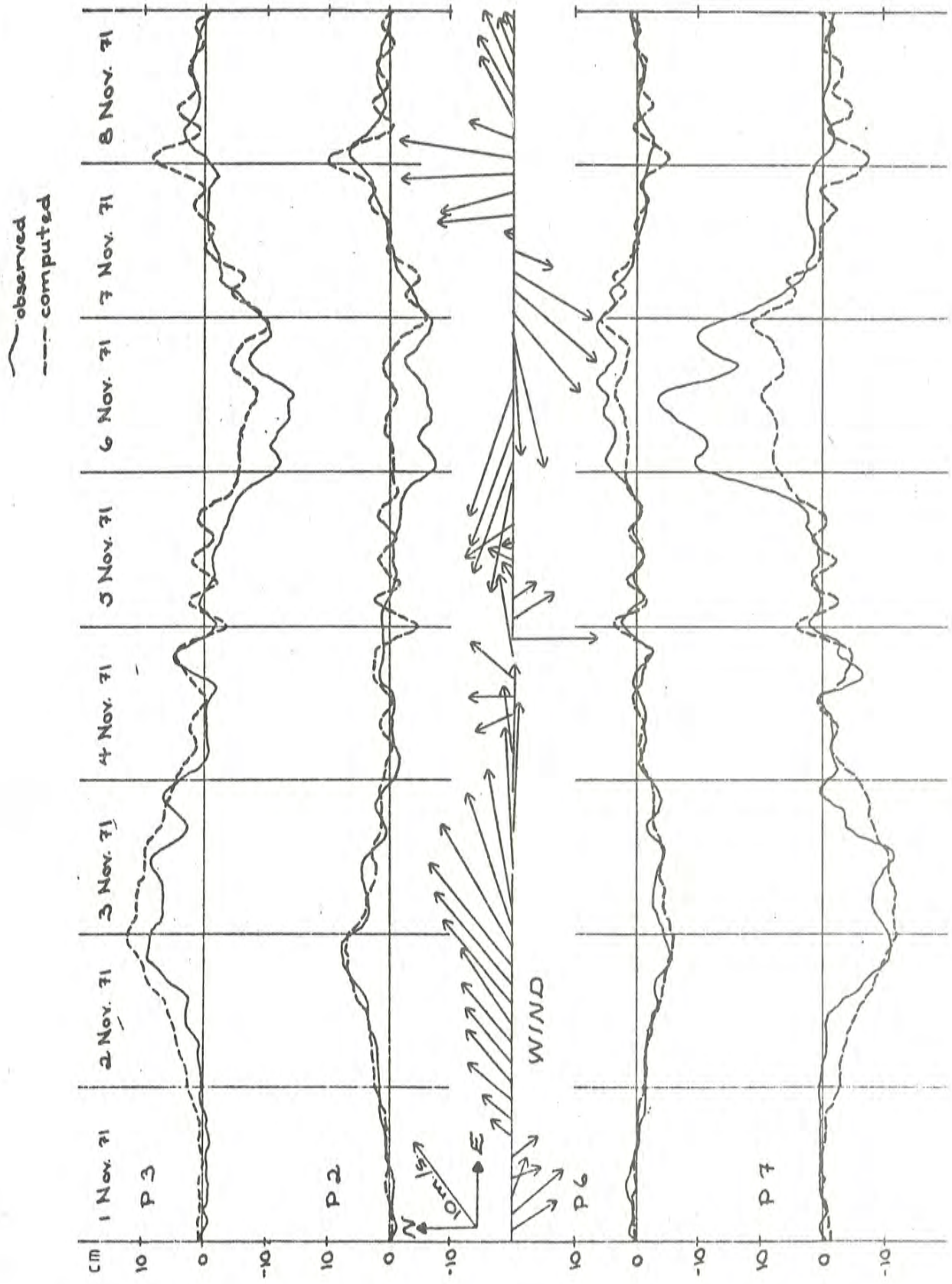

S M H I H B O	OBSERVED (SOLID LINES) AND COMPUTED (DASHED) CURRENTS FOR THE SURFACE LAYER AT TWO STATIONS DURING THE HOMOGENEOUS PERIOD	FIGURE 4 1971-11-01--08

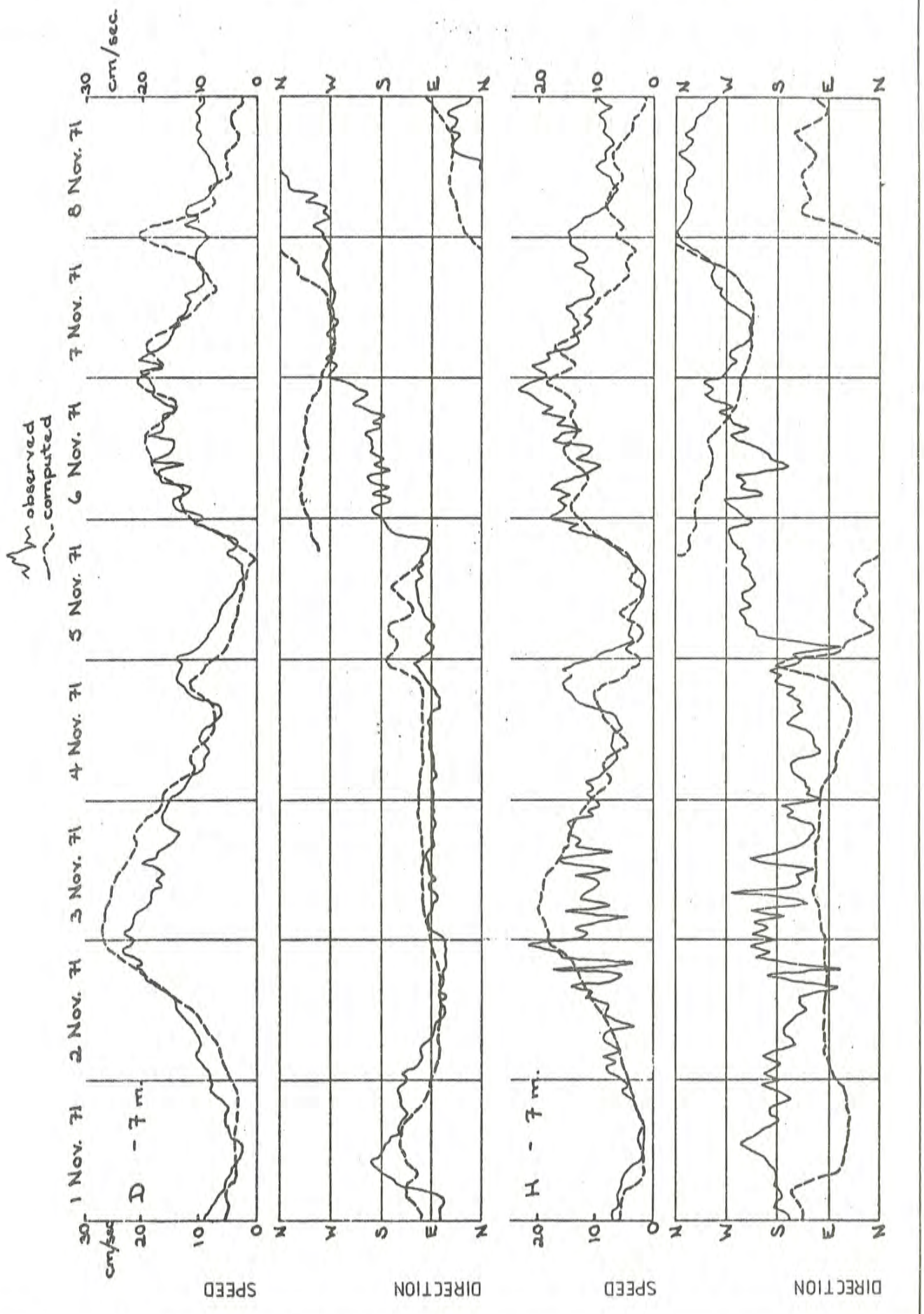

S M H I H B O	OBSERVED WINDS OVER LAKE VÄNERN DURING STRATIFIED MODELLING PERIOD (ABOVE), TOGETHER WITH A TYPICAL VERTICAL TEMPERATURE PROFILE USED AS INITIAL CONDITION (BELOW)	FIGURE 5 1971-08-26--09-04

OBSERVED WINDS FOR AREA 3

6-HOURLY VALUES

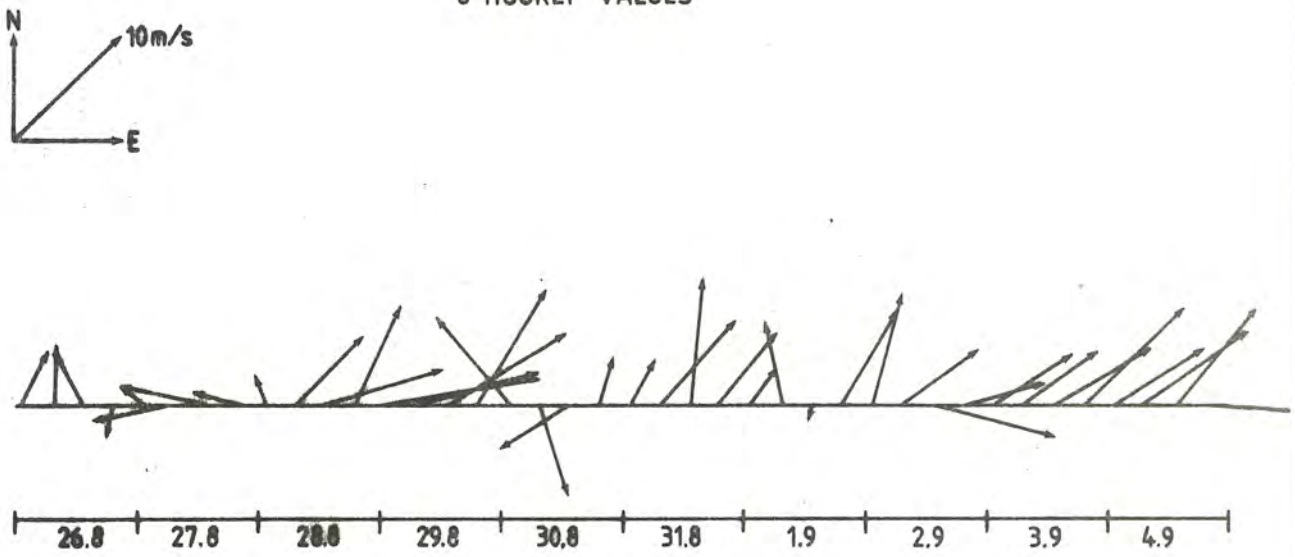

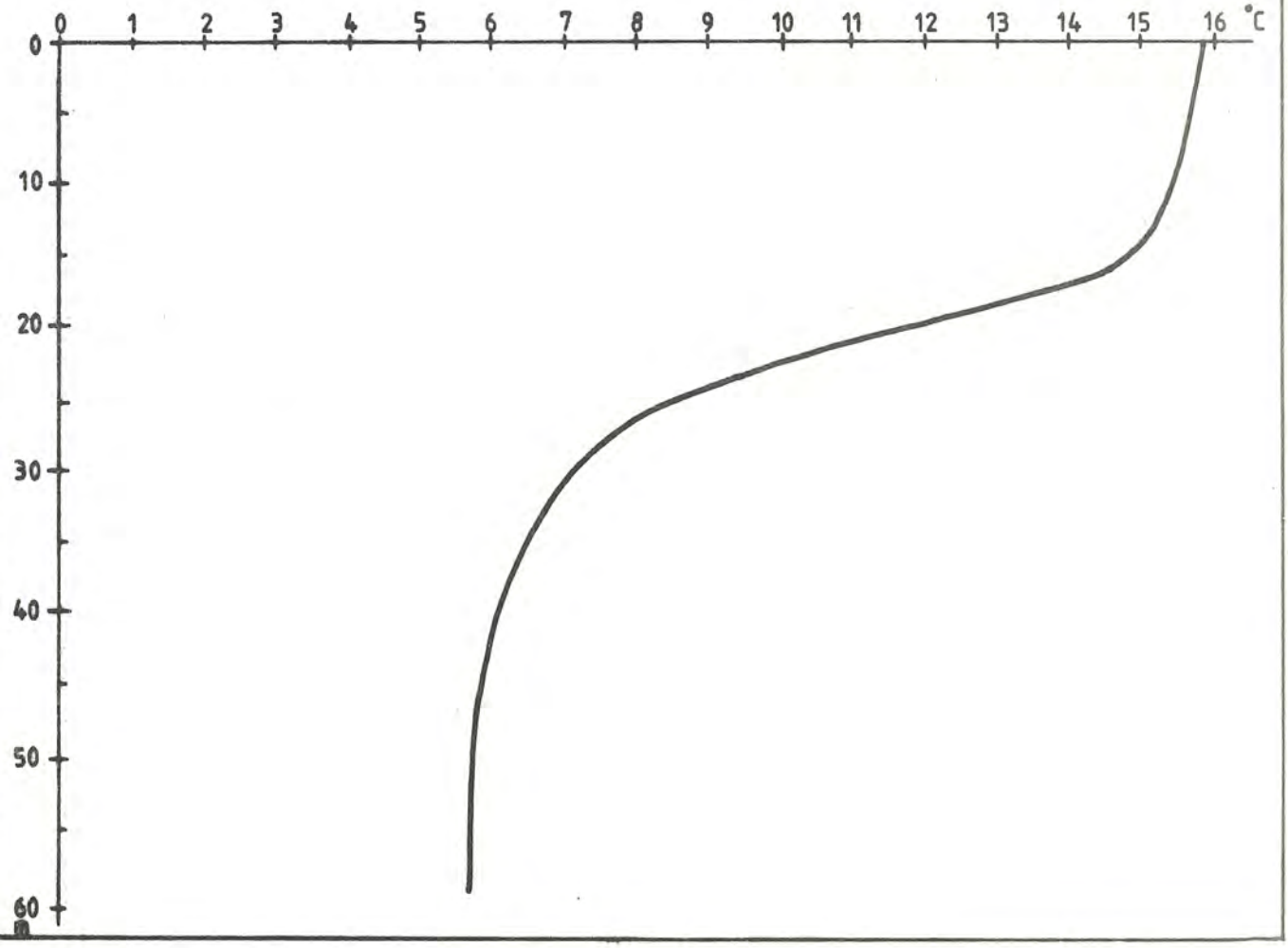

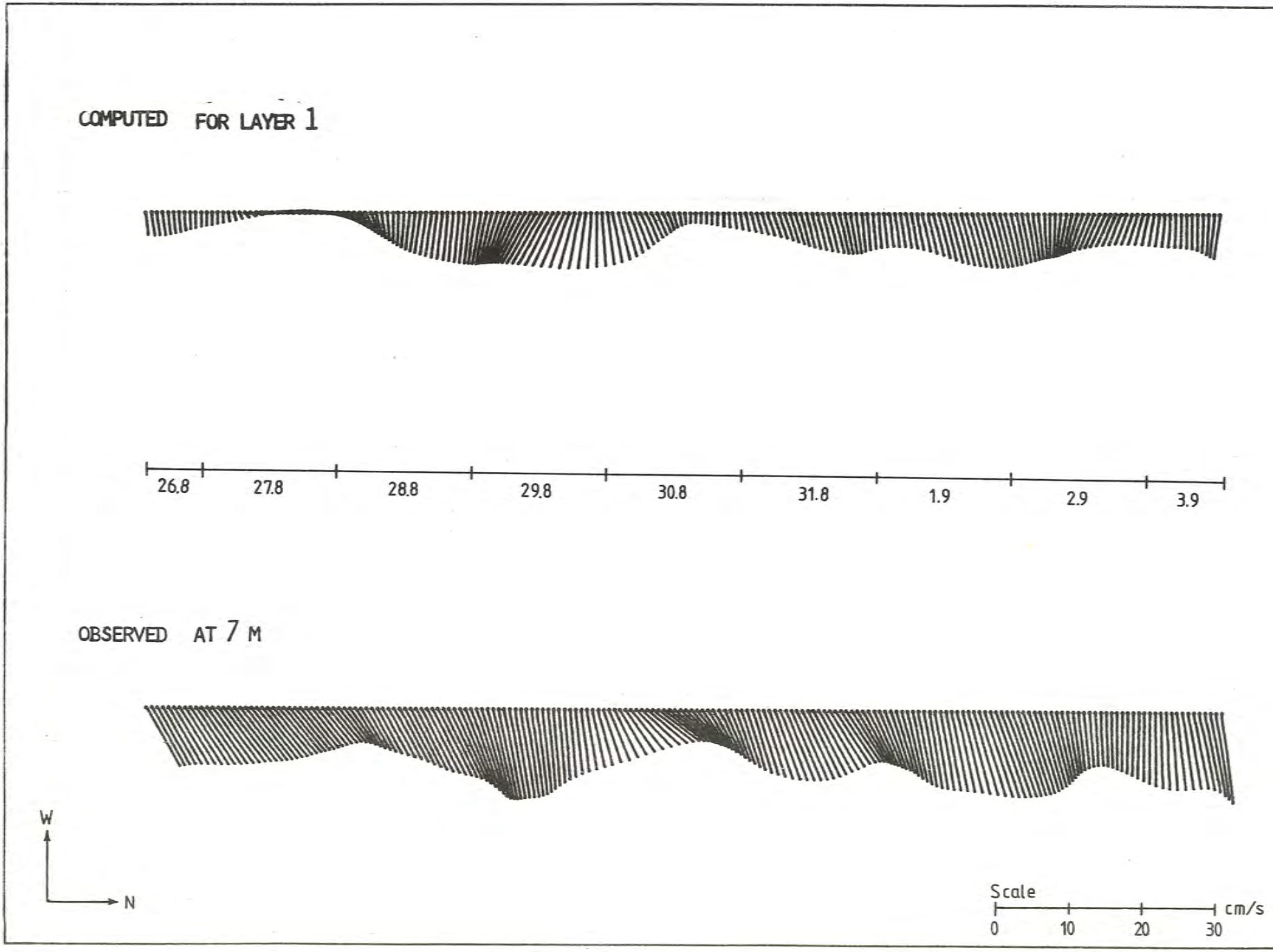

SMHI
HBO

COMPUTED AND OBSERVED CURRENTS FOR STATION D DURING STRATIFIED MODELLING PERIOD

1971-08-26--09-03

FIGURE 6 A

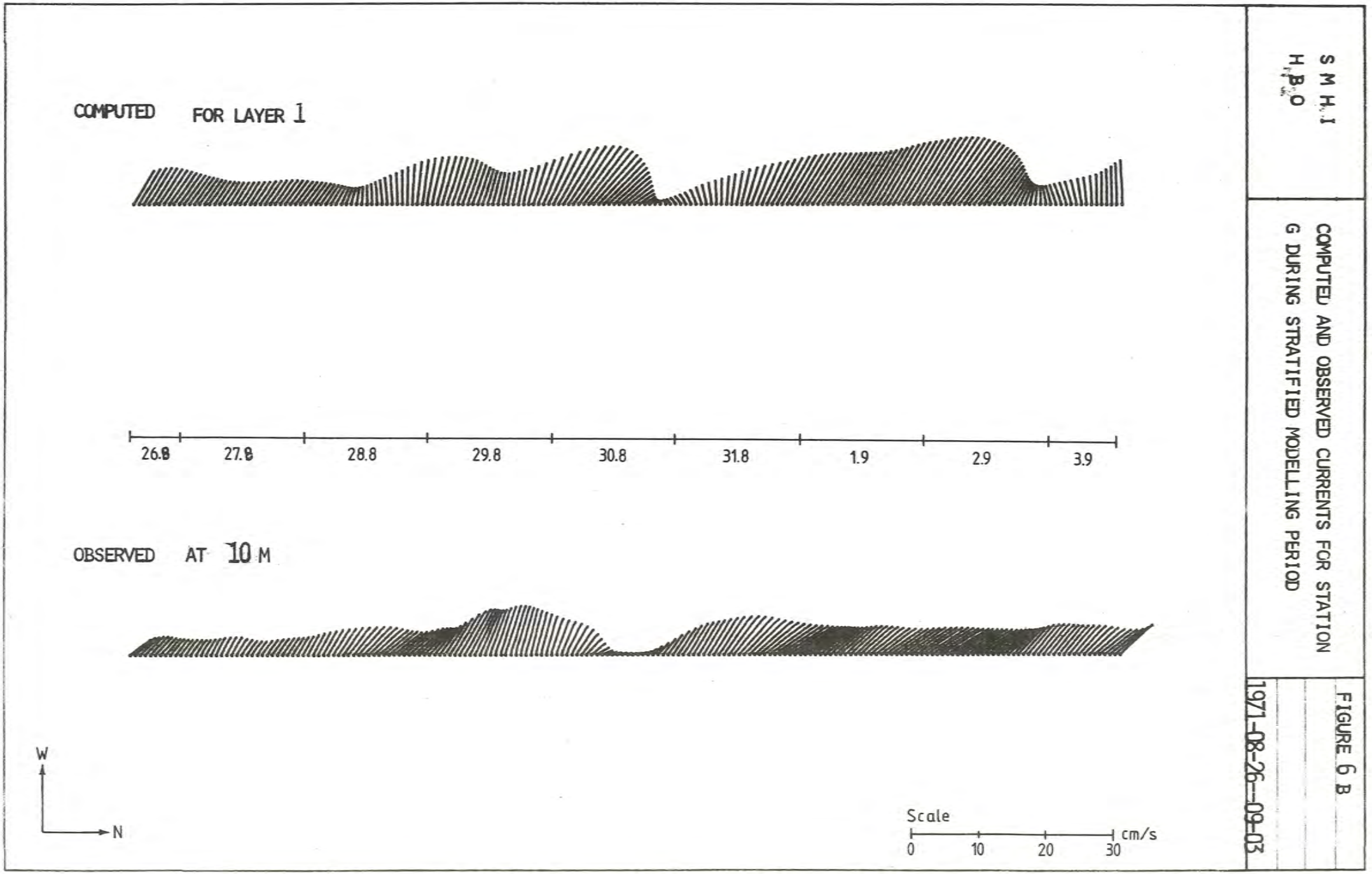

S M H I
H B O

COMPUTED AND OBSERVED CURRENTS FOR STATION G DURING STRATIFIED MODELLING PERIOD

1971-08-26--09-03

FIGURE 6 B

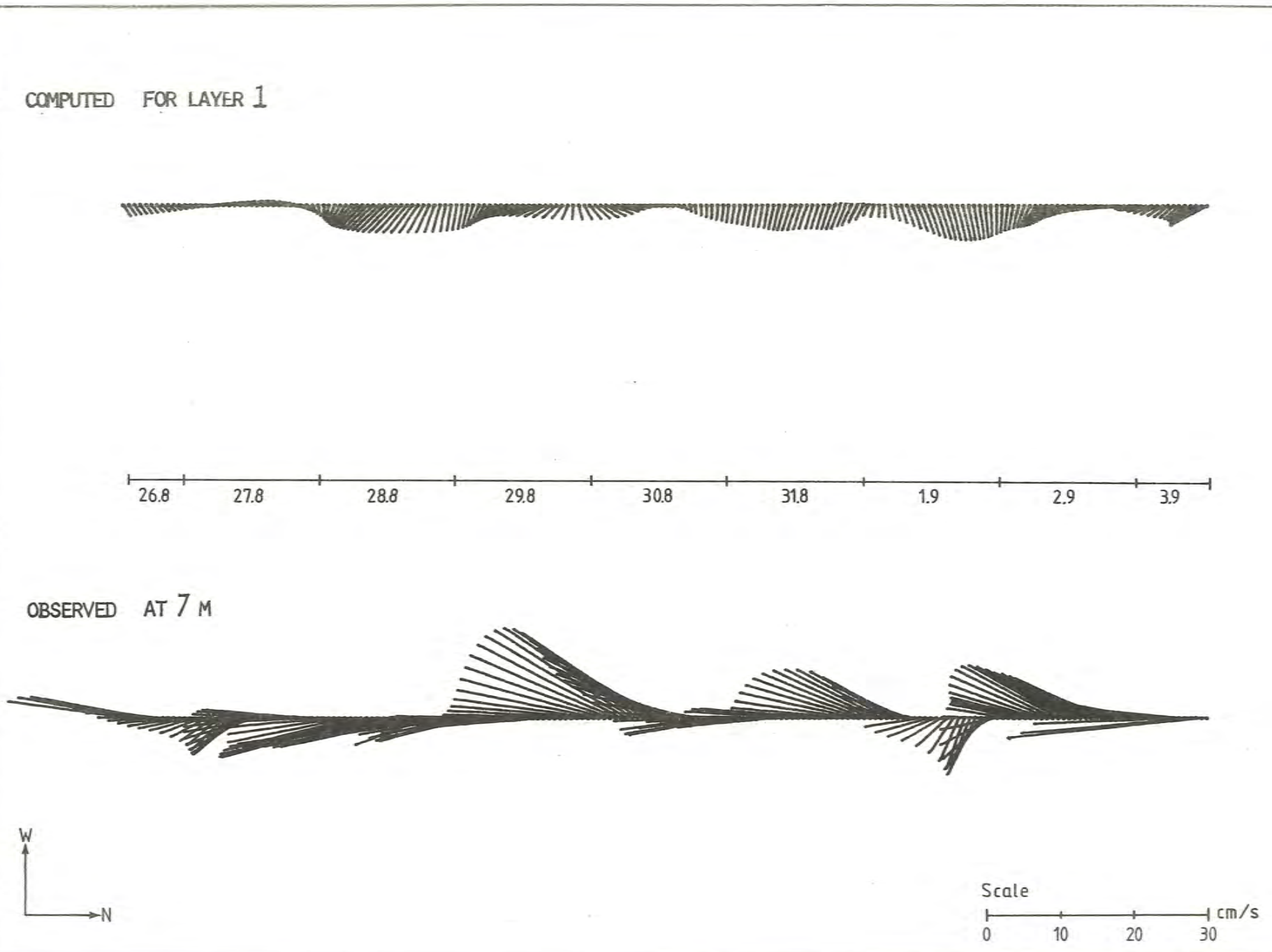

SMHI
HBO

COMPUTED AND OBSERVED CURRENTS FOR STATION C DURING STRATIFIED MODELLING PERIOD

1971-08-26--09-03

FIGURE 6 C

SMHI HBO	SYNOPTIC MAP OF COMPUTED CURRENTS FOR LAYER 1 (0-10 M) AT TIME 00.00. OBSERVED CURRENTS AT 7 M SHOWN BY HEAVY ARROWS	FIGURE 7A 1971-09-01

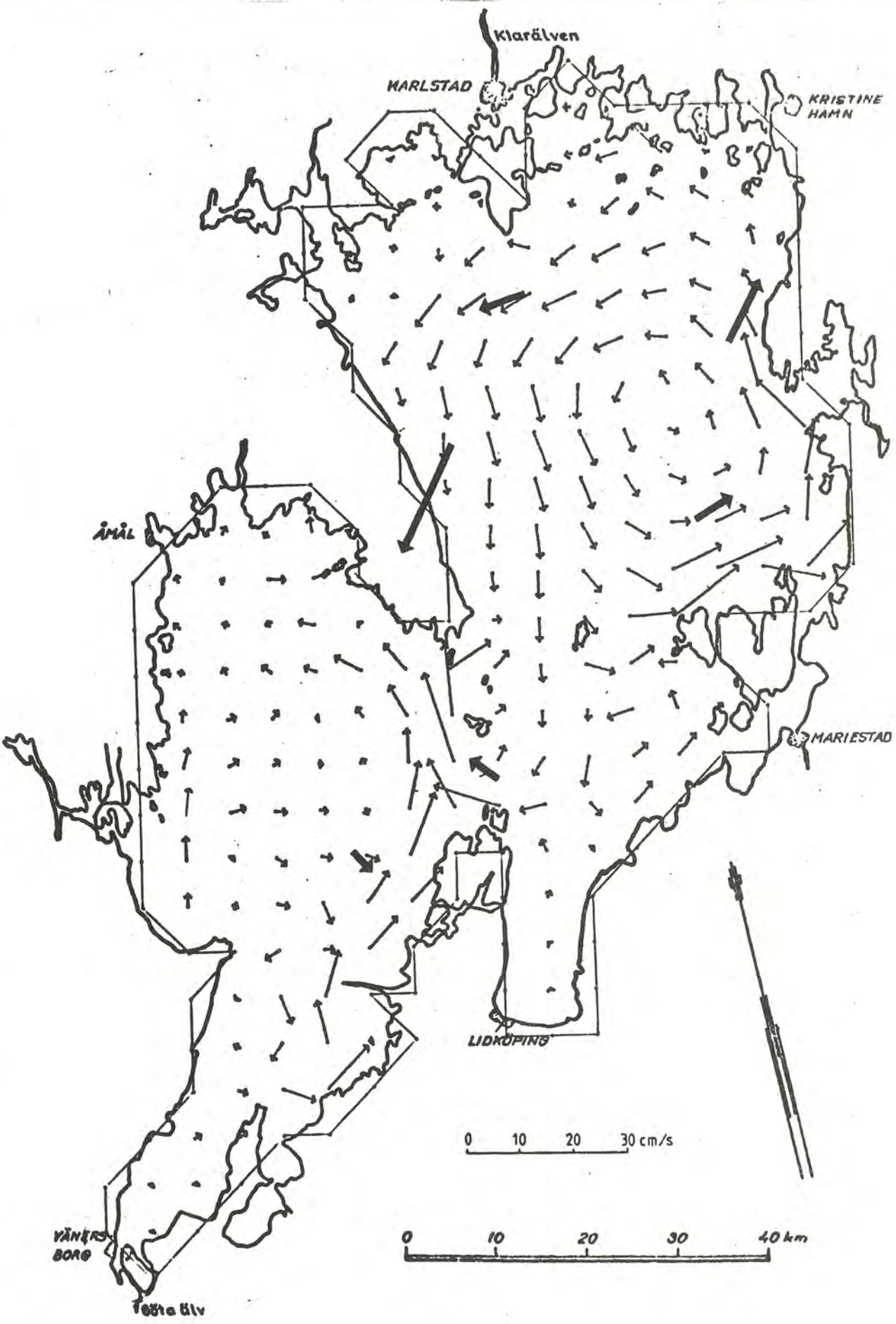

SMHI HBO	SYNOPTIC MAP OF COMPUTED CURRENTS FOR LAYER 3 (20-35 M) 1971-09-01 AT TIME 00.00. OBSERVED CURRENTS AT 25 M SHOWN BY HEAVY ARROWS	FIGURE 7B

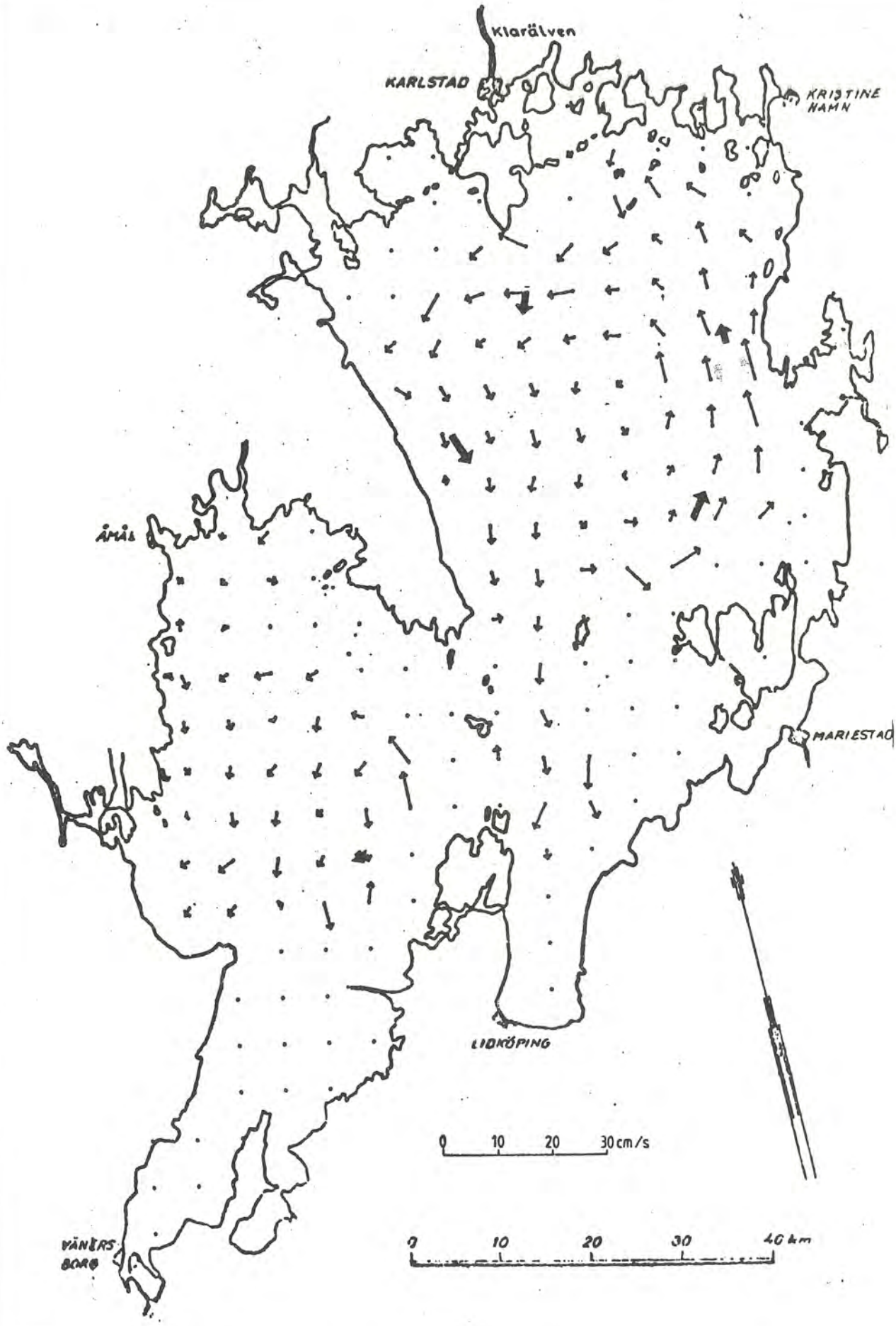

SMHI HBO	OBSERVED AND COMPUTED TEMPERATURES AT 25 M DEPTH FOR STATIONS IN EASTERN PART OF LAKE VÄNERN	FIGURE 8 1971-08-26--09-04

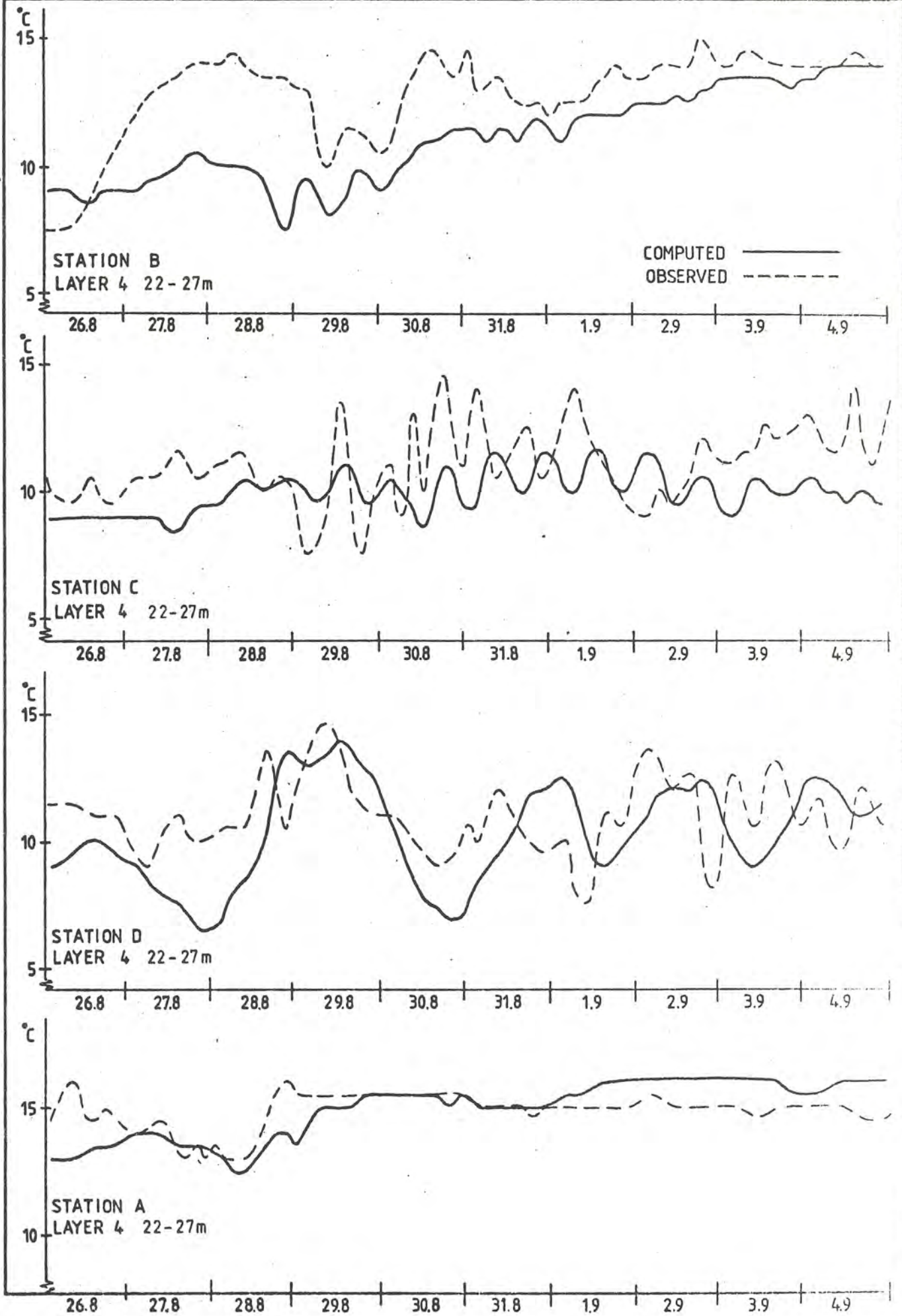

S M H I H B O	ABOVE: OBSERVED HIGH PASS CURRENT FOR UPPER LEVEL OF STATION B. BELOW: CORRESPONDING MODEL RESULTS FOR VERTICAL EDDY VISCOSITY OF 50 cm²/sec (SOLID LINE) AND 10 cm²/sec (DASHED LINE). COMPARE TABLE 1, RUNS 2 AND 3, RESPECTIVELY	FIGURE 9 1971-08-26--09-04

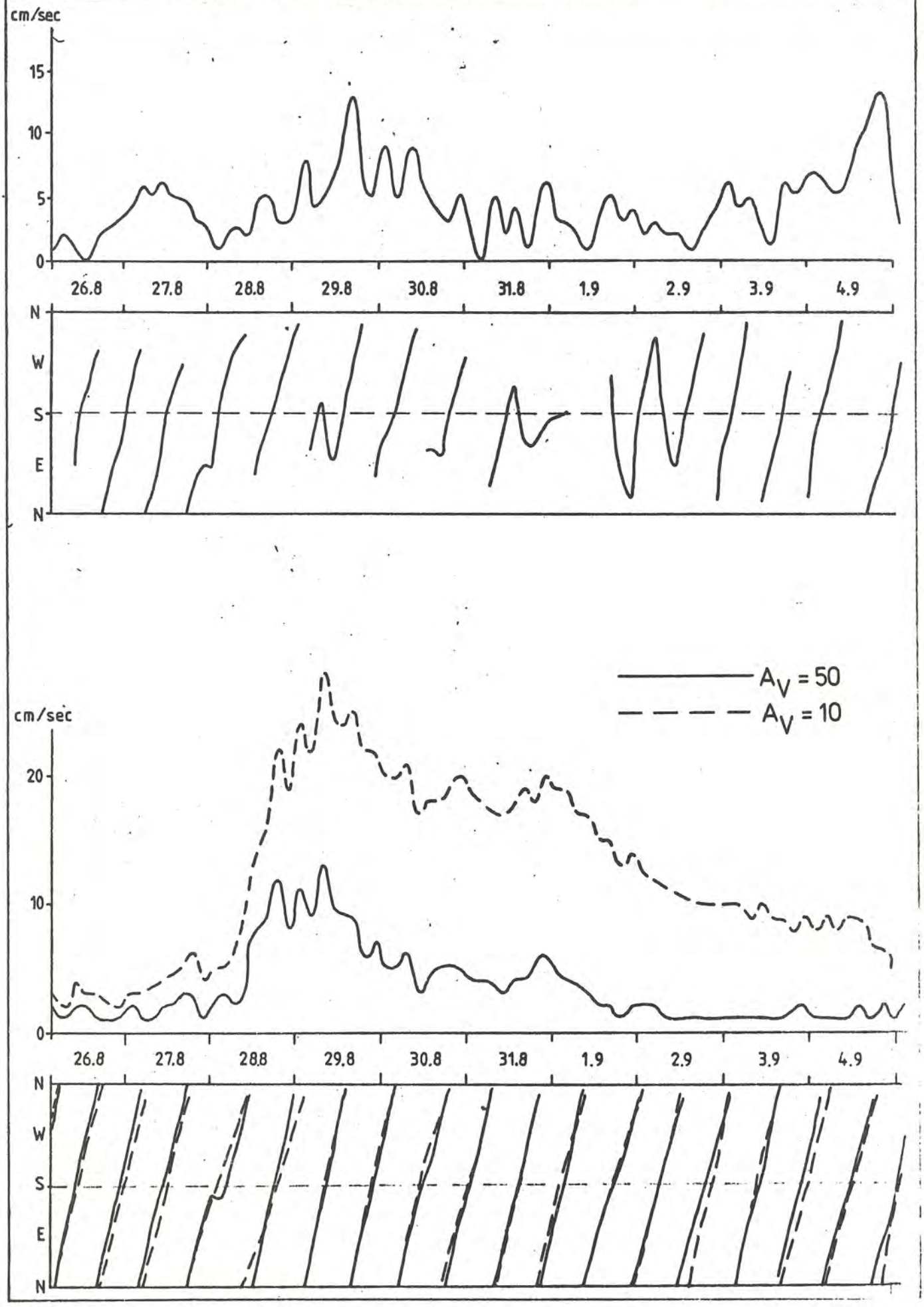

S M H I H B O	ABOVE: OBSERVED HIGH PASS CURRENT FOR UPPER LEVEL OF STATION C AT 25 M DEPTH. BELOW: CORRESPONDING MODEL RESULTS FOR VERTICAL EDDY VISCOSITY OF 50 cm²/sec (SOLID LINE) AND 10 cm²/sec (DASHED LINE). COMPARE TABLE 1 RUNS 2 AND 3.	FIGURE 10 1971-08-26--09-04

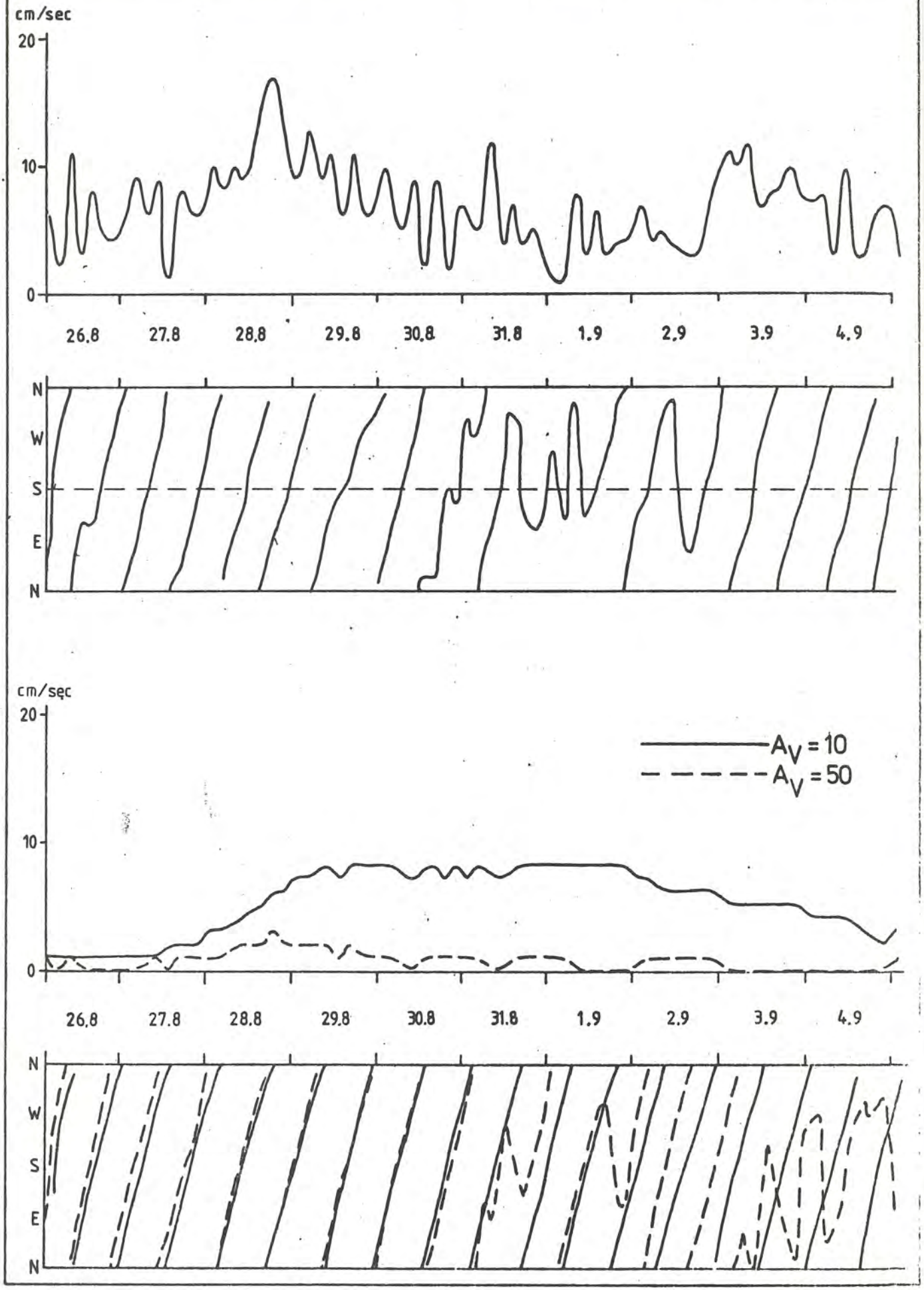

S M H I H B O	ABOVE: OBSERVED LOW PASS CURRENT FOR STATION C AT DEPTH 7 M. BELOW: CORRESPONDING MODEL RESULT OBTAINED FROM A DOUBLE LATTICE (SOLID LINE) AND A SINGLE LATTICE GRID (DASHED LINE) SEE RUNS 2 AND 8 OF TABLE 1.	FIGURE 11 1971-08-26--09-04

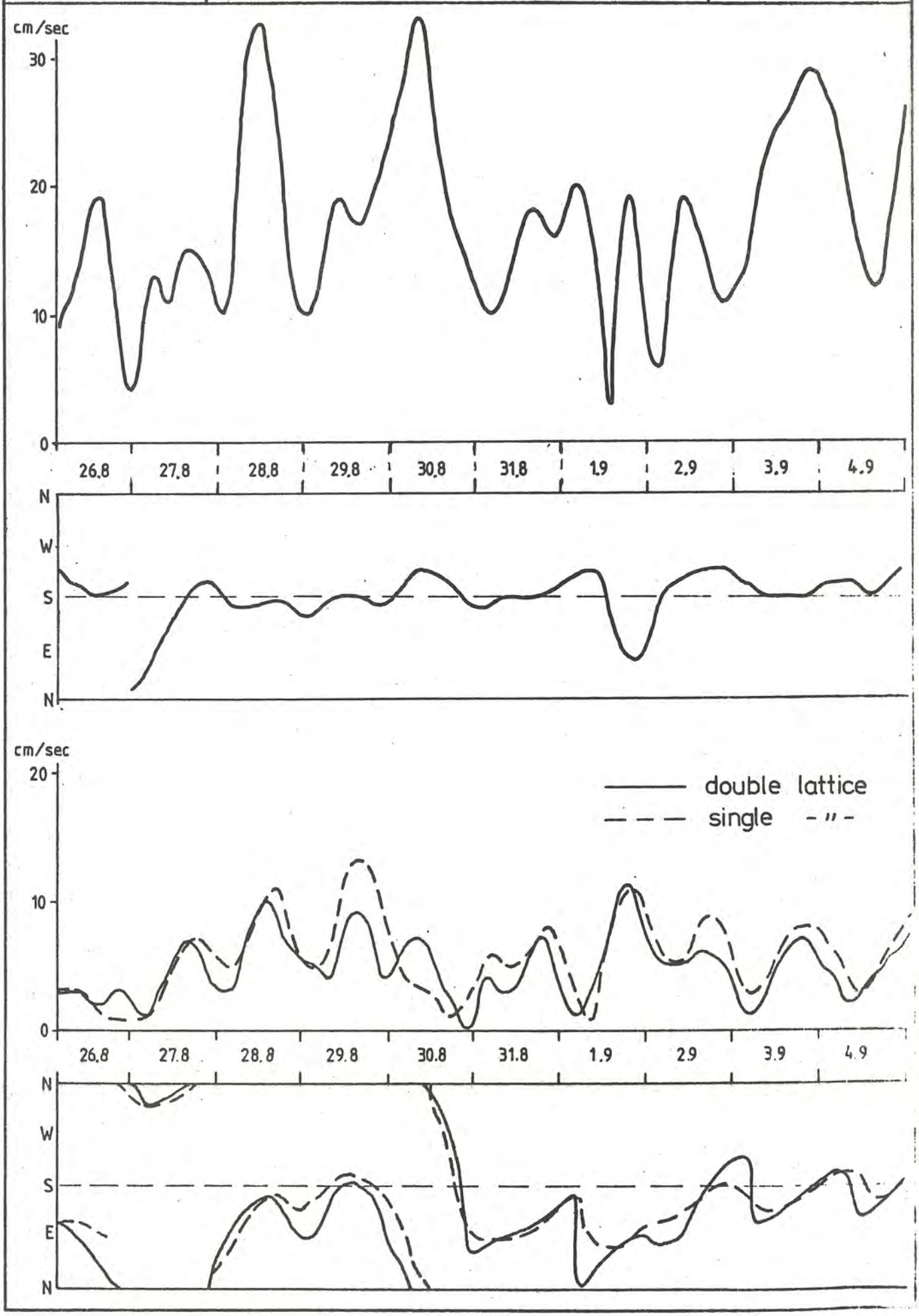

S M H I H B O	SAME STATION AS FIG 11 BUT MODEL RESULTS OBTAINED WITH AND WITHOUT HORIZONTAL EDDY VISCOSITY (ABOVE) AND FOR HIGH AND LOW VERTICAL EDDY VISCOSITY (BELOW), COMPARE RUNS 9, 10, 11 OF TABLE 1.	FIGURE 12 1971-08-26--09-04

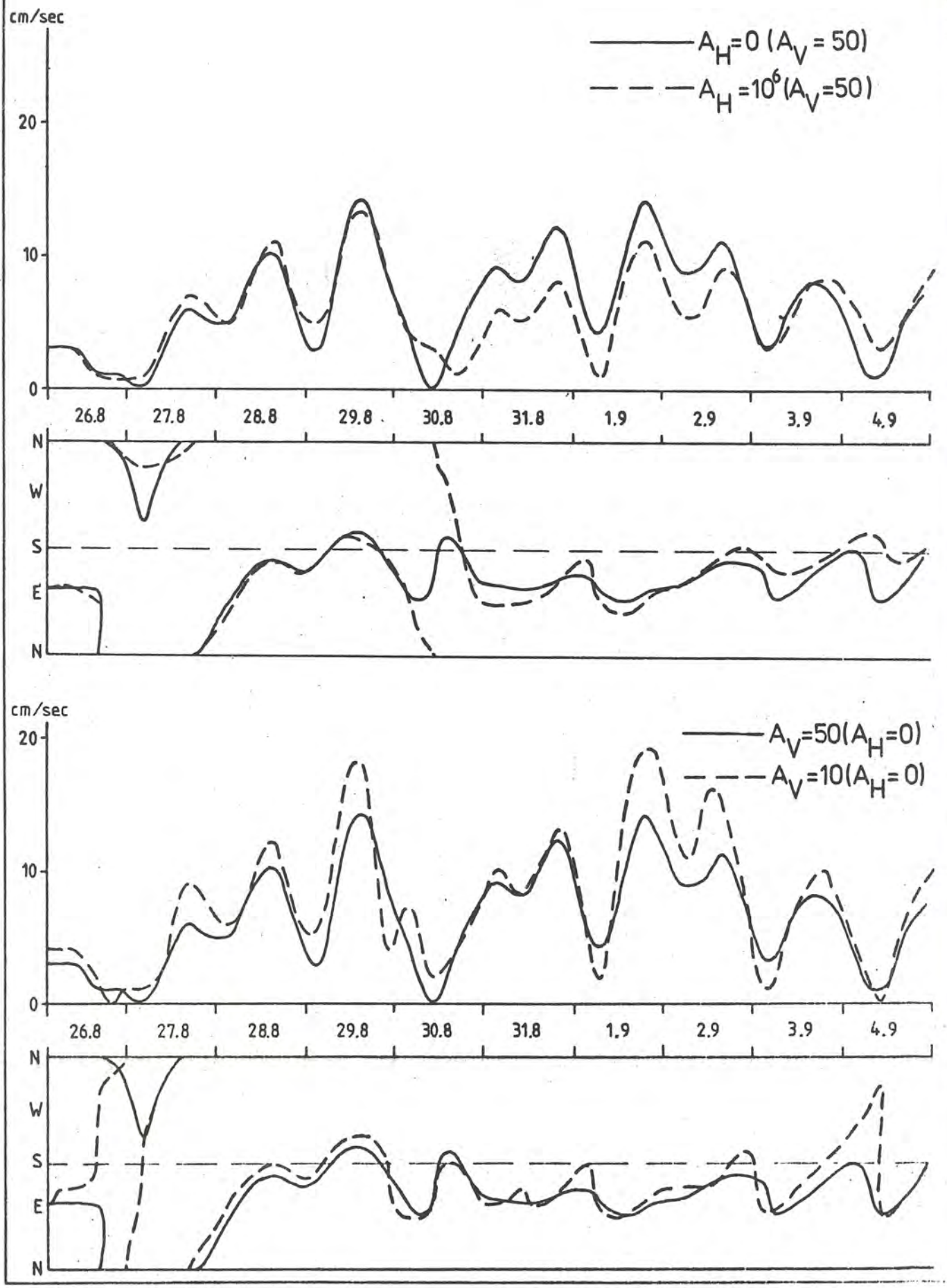

S M H I H B O	TEMPERATURE PREDICTIONS FOR STATION C OBTAINED FROM A 4-LAYER MODEL AND AN 8-LAYER MODEL. SEE TABLE 1, RUNS 11 AND 13.	FIGURE 13 1971-08-26--09-04

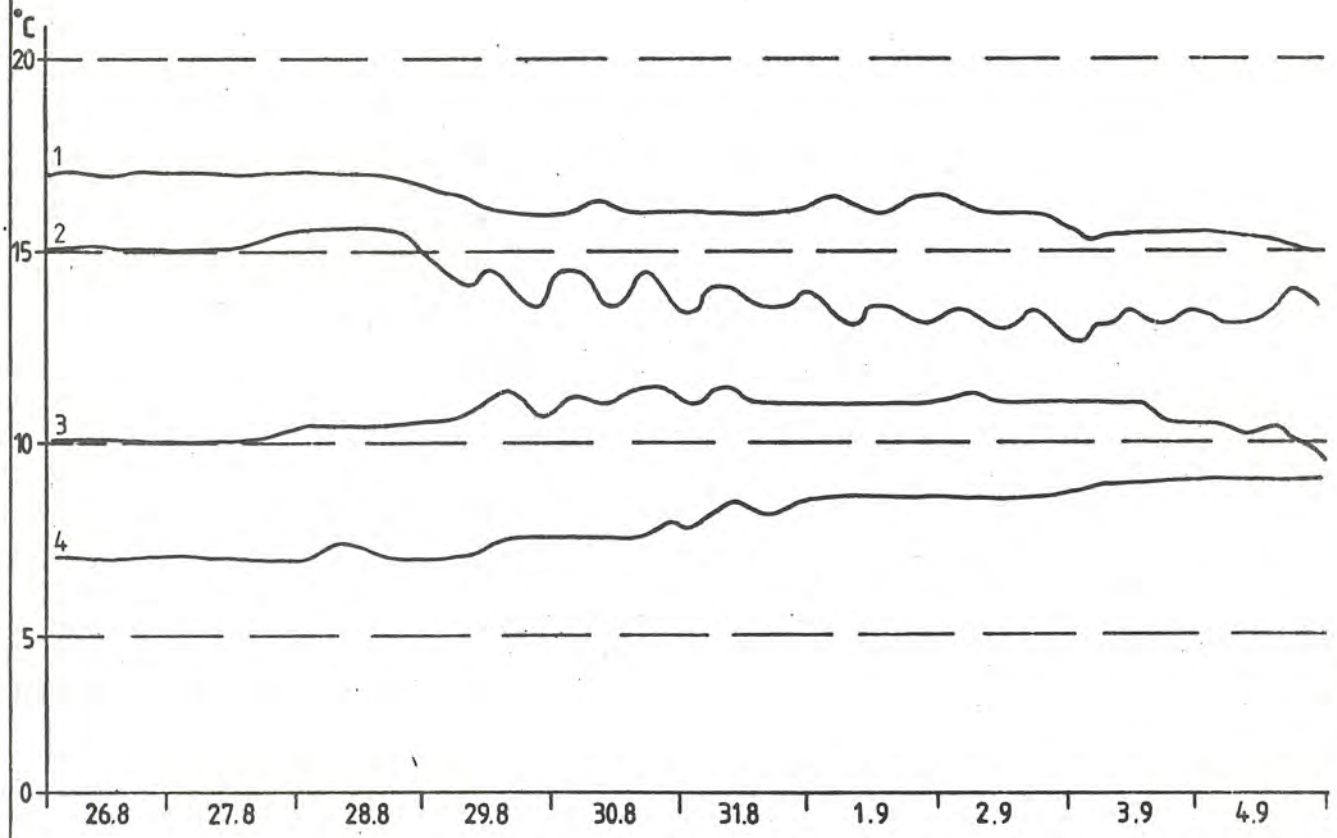

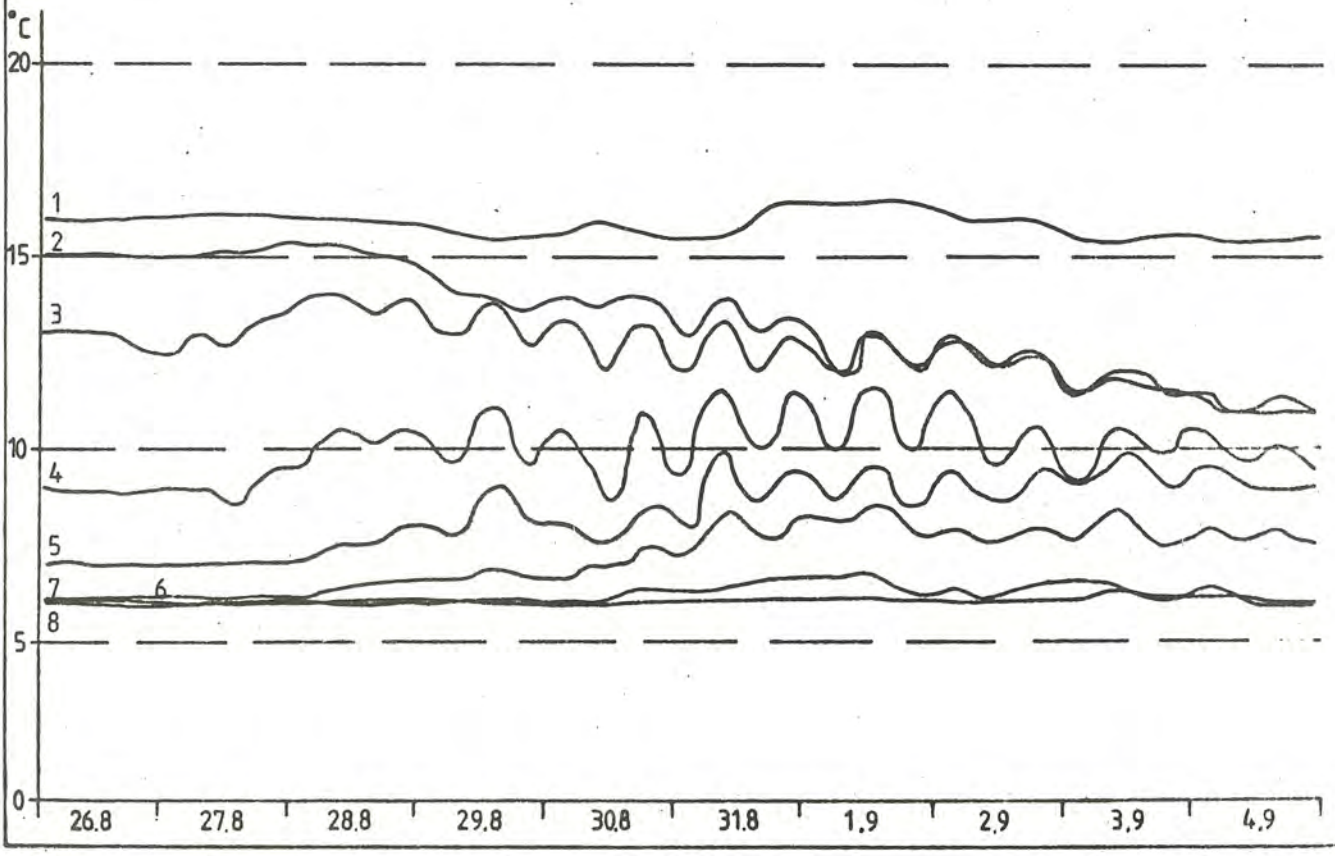

Notiser och preliminära rapporter

Serie HYDROLOGI

Nr 1 Sundberg-Falkenmark M
Om isbärighet. Stockholm 1963

Nr 2 Forsman, A
Snösmältning och avrinning. Stockholm 1963

Nr 3 Karström, U
Infrarödteknik i hydrologisk tillämpning: Värmebilder som hjälpmedel i recipientundersökningar. Stockholm 1966

Nr 4 Moberg, A
Svenska sjöars isläggnings- och islossningstidpunkter 1911/12-1960/61. Del 1. Redovisning av observationsmaterial. Stockholm 1967

Nr 5 Ehlin, U & Nyberg, L
Hydrografiska undersökningar i Nordmalingsfjärden. Stockholm 1968

Nr 6 Milanov, T
Avkylningsproblem i recipienter vid utsläpp av kylvatten. Stockholm 1969

Nr 7 Ehlin, U & Zachrisson, G
Spridningen i Vänerns nordvästra del av suspenderat materiel från skredet i Norsälven i april 1969. Stockholm 1969

Nr 8 Ehlert, K
Mälarens hydrologi och inverkan på denna av alternativa vattenavledningar från Mälaren. Stockholm 1970

Nr 9 Ehlin, U & Carlsson, B
Hydrologiska observationer i Vänern 1959-1968 jämte sammanfattande synpunkter. Stockholm 1970

Nr 10 Ehlin, U & Carlsson, B
Hydrologiska observationer i Vänern 17-21 mars 1969. Stockholm 1970

Nr 11 Milanov, T
Termisk spridning av kylvattenutsläpp från Karlshamnsverket. Stockholm 1971

Nr 12 Persson, M
Hydrologiska undersökningar i Lappträskets representativa område. Rapport I. Stockholm 1971

Nr 13 Persson, M
Hydrologiska undersökningar i Lappträskets representativa område. Rapport II. Snömätningar med snörör och snökuddar Stockholm 1971

Nr 14 Hedin, L
Hydrologiska undersökningar i Velens representativa område. Beskrivning av området, utförda mätningar samt preliminära resultat. Rapport I. Stockholm 1971

Nr 15 Forsman, A & Milanov, T
Hydrologiska undersökningar i Velens representativa område. Markvattenstudier i Velenområdet. Rapport II. Stockholm 1971

Nr 16 Hedin, L
Hydrologiska undersökningar i Kassjöåns representativa område. Nederbördens höjdberoende samt kortfattad beskrivning av området. Rapport I. Stockholm 1971

Nr 17 Bergström, S & Ehlert, K
Stochastic Streamflow Syntheses at the Velen representative Basin. Stockholm 1971

Nr 18 Berström, S
Snösmältningen i Lappträskets representativa område som funktion av lufttemperaturen. Stockholm 1972

Nr 19 Holmström, H
Test of two automatic water quality monitors under field conditions. Stockholm 1972

Nr 20 Wennerberg, G
Yttemperaturkartering med strålningstermometer från flygplan över Vänern under 1971. Stockholm 1972

Nr 21 Prych, A
A warm water effluent analyzed as a buoyant surface jet. Stockholm 1972

Nr 22 Bergström, S
Utveckling och tillämpning av en digital avrinningsmodell. Stockholm 1972

Nr 23 Melander, O
Beskrivning till jordartskarta över Lappträskets representativa område. Stockholm 1972

Nr 24 Persson, M
Hydrologiska undersökningar i Lappträskets representativa område. Rapport III. Avdunstning och vattenomsättning. Stockholm 1972

Nr 25 Häggström, M
Hydrologiska undersökningar i Velens representativa område. Rapport III. Undersökning av torrperioderna under IHD-åren fram t o m 1971. Stockholm 1972

Nr 26 Bergström, S
The application of a simple rainfall-runoff model to a catchment with incomplete data coverage. Stockholm 1972

Nr 27 Wändahl, T & Bergstrand, E
Oceanografiska förhållanden i svenska kustvatten. Stockholm 1973

Nr 28 Ehlin, U
Kylvattenutsläpp i sjöar och hav. Stockholm 1973

Nr 29 Andersson, U-M & Waldenström, A
Mark- och grundvattenstudier i Kassjöåns representativa område. Stockholm 1973

Nr 30 Milanov, T
Hydrologiska undersökningar i Kassjöåns representativa område. Markvattenstudier i Kassjöåns område. Rapport II. Stockholm 1973

SMHI Rapporter

HYDROLOGI OCH OCEANOGRAFI

Nr RHO 1
Weil, J G
Verification of heated water jet numerical model
Stockholm 1974

Nr RHO 2
Svensson, J
Calculation of poison concentrations from a hypothetical accident off the Swedish coast
Stockholm 1974

Nr RHO 3
Vasseur, B
Temperaturförhållanden i svenska kustvatten
Stockholm 1975

Nr RHO 4
Svensson, J
Beräkning av effektiv vattentransport genom Sunninge sund till Byfjorden
Stockholm 1975

Nr RHO 5
Bergström, S & Jönsson, S
The application of the HBV runoff model to the Filefjell research basin
Norrköping 1976

Nr RHO 6
Wilmot, W
A numerical model of the effects of reactor cooling water on fjord circulation
Norrköping 1976

Nr RHO 7
Bergström, S
Development and Appl. of a Conceptual Runoff Model
Norrköping 1976

Nr RHO 8
Svensson, J
Seminars at SMHI 1976-03-29--04-01 on Numerical Models of the Spreading of Cooling-water
Norrköping 1976

Nr RHO 9
Simons, J & Funkquist, L & Svensson, J
Application of a numerical model to Lake Vänern
Norrköping 1977